ROYAL SOCIETY OF CHEMISTRY

www.rsc.org/crystengcomm

Graphical contents entry

Functional Shakeup of Metal-Organic Frameworks: the Rise of the Sidekick

Jun He,[a] Matthias Zeller,[b] Allen D. Hunter,[b] and Zhengtao Xu*[,c]

Ever more versatile side groups—from labile, weak donors to strong-binding thiol and dendritic functions, sulfur-enabled framework chemistry heralds a rising trend in the design of solid state materials.

Journal Name

ARTICLE

Functional Shakeup of Metal-Organic Frameworks: the Rise of the Sidekick

Jun He,[a] Matthias Zeller,[b] Allen D. Hunter,[b] and Zhengtao Xu*[c]

Merging is the simple term that captures the spirit of this essay. This refers to merging, both structurally and functionally, the distinct moieties of the backbone and the side group in the topical design of the porous solids of metal-organic frameworks (MOFs). As the backbone has been traditionally the focus of study, the merging translates into a rise of the side group functions, which have of late proven increasingly important for functionalizing the porous grid. The wide range of usable organic side groups, however, also presents a paradox of choice. Instead of mechanically latching side groups onto the backbone (i.e., with their innate, solution–phase reactivity more or less retained), we focus on distinct, dramatic synergism. Distinct being a subjective term open to dispute, we specify two modes of merging/integrating. One regards the unconventional, backfolded shape of the ligand, in which rigid side arms coalesce with the backbones to generate multiple, pre-assembled subunits (i.e., the simple tritopic subunits), each of which conforms to the traditional starburst shape. The other mode of merging regards crosslinking the side groups, which broadly ranges from earlier use of simple σ bond links for mechanically locking in the MOF grid, to the more polarizable metal-chalcogenide or organic π bridges that stand to tranform the insulating MOF grid into next-generation solid state electronic materials.

Introduction

The sidekick here refers to the side groups attached to the backbones of molecular building blocks for functionalizing the prospective metal-organic frameworks as a surging class of porous crystalline materials.[1] Such side groups stand in contrast with the primary donor ends that are intended for bonding with metal ions to build up the framework. The metaphor here invokes two observations regarding the research of MOF materials.

The first one refers to the historically prominent position taken by the studies of rigid, polytopic molecules as building blocks for extended networks. In these studies, the attention is devoted to the backbone of the molecule and how its shape and size correlate with the resultant network topology and pore features. Notable examples include the tectonic design of Wuest (e.g., on H-bonded nets),[2] Robson's seminal diamond net (from coordinating Cu^{+} ions and a tetrapod ligand),[3] Lee and Moore's guest-exchange studies,[4] Kitagawa's early work on gas sorption,[5] and the Yaghi/O'Keeffe papers on reticular synthesis;[6] and exercises in this direction of backbone design and network synthesis remain active.[7] The functionalization by means of side groups, by comparison, was for a long time relegated to a lesser role, even though the idea had already

been intently pursued in the early stage of the game (e.g., Fig. 1).[8] The surging of the side groups in recent years has been spectacular, including the hydroxyl,[9] ether,[10] phosphine,[11] thioether,[12] thiol (-SH),[13] amino acid side chains and so on.[14] Overall, research along this line is necessarily driven by the rich array of versatile functionalities that can be accessed by synthetic molecular chemistry, giving rise to effective strategies for preventing interpenetration (i.e., via thermo- and photo-cleavable side groups),[15] as well as a wide range of other post-synthetic modifications.[16] Systematic classification of the various side groups (e.g., based on donor characteristics, or on the structural control vs reactivity/properties imparted), would be helpful, but entail a full-length review.

Our true intent in this brief Highlight, however, lies in a second observation. Unlike the above general observation about the research activities in the field, here we are pondering the relation between the backbone and side group within the technical realm of chemical functionality. The thought is about blurring the line between the backbone and the side group, and about merging the structural as well as the functional roles played by the backbone and the side group. By promoting the side group, we seek to impart a potentially subversive role to the side groups, and to shift the established order in network design. More broadly, such dichotomy also appeals to the imagination, as the human psyche invariably relishes stories of the underdog.

From stand-alone side groups to a memory net

[a] School of Chemical Engineering and Light Industry, Guangdong University of Technology, Guangzhou 510006, Guangdong, China
[b] Department of Chemistry, Youngstown State University, One University Plaza, Youngstown, OH 44555, USA
[c] Department of Biology and Chemistry, City University of Hong Kong 83 Tat Chee Avenue, Kowloon, Hong Kong, China. E-mail: zhengtao@cityu.edu.hk
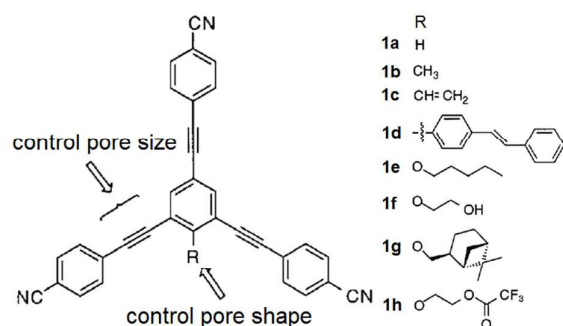
**Fig. 1** Bare backbone ligand **1a**, and derivatives (**1b**-**1h)** with single pendant side groups.

The division between the backbone and the side group was indeed distinct to begin with. In the initial design (Fig. 1), the side group was placed at a distance from the primary end groups (e.g., the –CN donors in Fig. 1), in order to minimize the impact on the network formation properties. As it were, the

series of ligands (**1a**-**1h**) persistently formed into honeycomb-channeled nets via the coordination with 3-connected Ag(I) ions; whereas the side groups remain free-standing pendants in the pores.

Also, in this early orthogonal design, the attachment of the side group is rather mechanical, with relatively little interaction with the backbone to generate new chemical/physical properties, properties that would help to highlight a more impressive role of the side group. The chemical identity of the side groups, for example, remains quite similar to that in the solution phase. To be sure, context always matters—a group on the solid grid is, after all, no longer a group in solution. In deliberating the novelty of properties, the emphasis here is necessarily on a matter of degree rather than kind. The more pragmatic intent, on the other hand, remains to sharpen the focus on chemical functions of distinctive, deeper importance.
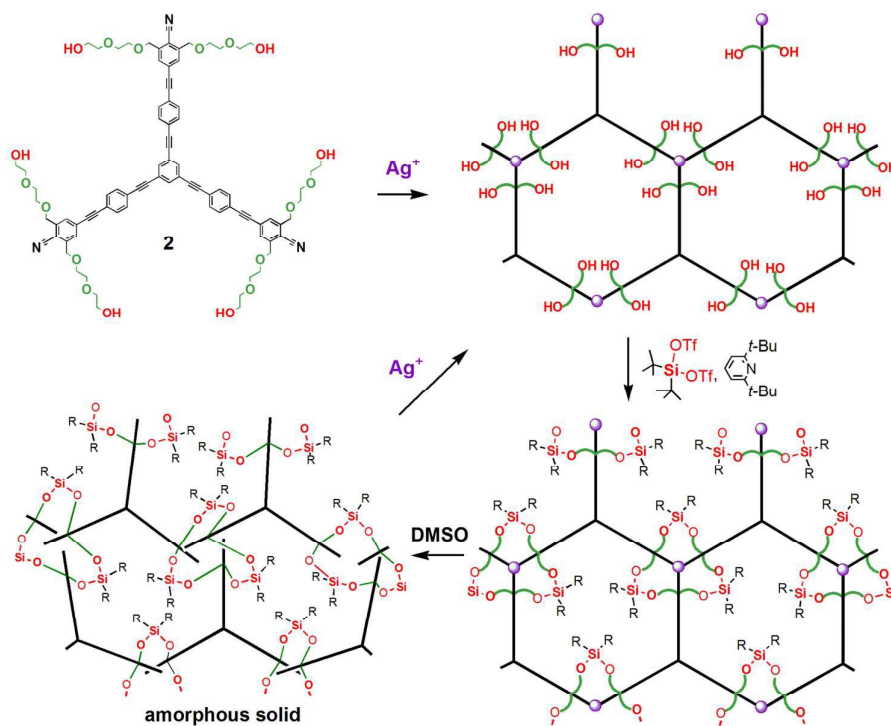
Fig. 2 Dendritic ligand **2** with tritopic nitrile backbone and six floppy, hydroxyl-ended side chains (top left), and the assembly into a crystalline honeycomb net (schematically shown in top right) based nitrile-Ag(I) coordination, followed by three further transformations: crosslinking the hydroxyl side chains by a silyl ditriflate agent yields a covalent solid retaining the initial crystalline order (lower right); subsequent extraction of the Ag(I) ions by dimethyl sulfoxide (DMSO) yields an amorphous, polymeric solid (lower left), which can nevertheless pick Ag(I) ions from a solution and regain the order dictated by the initial coordination net.

ARTICLE
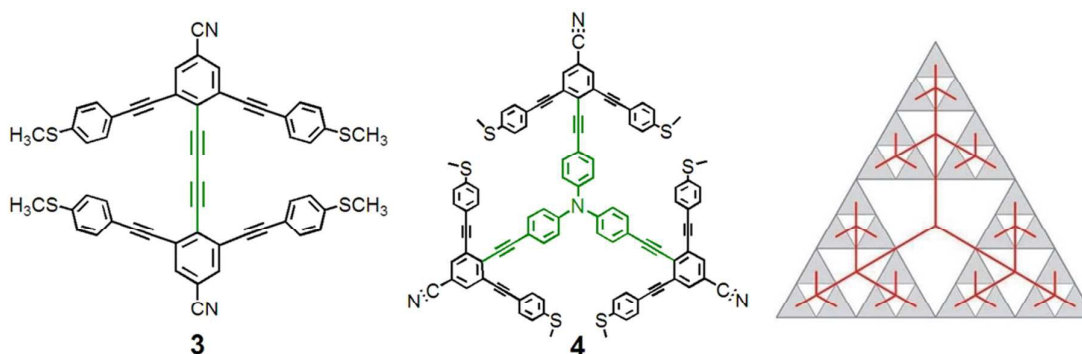
Fig. 3 Backfolded molecules **3** and **4**, and a Sierpinski triangle (with the geometrically equivalent ternary tree shown in red)**.** Molecule **4** compares well with the Sierpinski triangle, but contrasts with the above **2** molecule, which has flexible side chains and can take a radiant form that is geometrically different. The backfolded molecules **3** and **4** can be deconstructed into tritopic subunits preassembled by the core fragments (shown in green).

Let us use a concrete discovery to illustrate the somewhat subtle argument about interaction and novelty. As seen in Fig. 2, the extensive, symmetrical presence of side chains in molecule **2** gives a more imposing look of a dendrimer. The persistent formation of the honeycomb net, upon crystallizing with Ag(I) ions, can be ascribed to the soft natures of the –CN and Ag(I) species, as well as the reduced interfacial energy afforded by the honeycomb pattern.[8c, 17] So far the division of labor between backbone and the side chains remains clear. Crosslinking by the silyl ditriflate agent, however, brings the side chain functions to the fore: they morphed from appended side groups into crucial bridges; and the whole structure consequently transforms from a fragile coordination net into a covalent, polymeric grid. The impacts on properties are no less dramatic: the crosslinked, crystalline scaffold can be deprived of the Ag(I) ions (by soaking in DMSO), giving an amorphous powder that nevertheless retains a precise memory of structure: i.e., a memory by which re-insertion of Ag(I) ions readily recovers the crystalline order of the original net. Such dynamic structural changes in the solid state are clearly beyond the respective reaches of coordination networks and traditional polymers, highlighting a unique synergism arising from the strength of the crosslinked side groups being fully merged with the directional order initially laid out by the rigid backbone.

Backfolded shape integrates the side arms

Besides network dynamics and transformation, the subversive role of the side groups can also be fulfilled in the more static realm of structural and topology analysis. The symmetrically back-folded molecules of **3** and **4** (Fig. 3) present a case in point.[18] The attachment of the rigid side arms, with their terminal thioether donors, greatly diminishes the ditopic character of the cyano groups on the backbone in **3**: so much so that the molecule as a whole can be deconstructed into two tritopic subunits preassembled by the diacetylene fragment (shown in green in Fig. 3).

In **4**, the six side arms, installed on the tritopic backbone, deal a structural impact that is even more dramatic: here we are presented with a supertritopic, self-similar motif[18b] that is geometrically equivalent to the famous Sierpinski triangle as shown in the right panel of Fig. 3. In this fractal-like, hierarchical molecule, tritopic shapes on two orders can be identified: the three primary (-CN) branches constitutes the 1st order; each of the individual –CN branches and the two MeS-side arms form the 2nd order.

These backfolded molecules are thus seen to differ geometrically—on a fundamental level--from conventional dendrimers, in which the branches can be pointed outward in a starburst form. As a norm, it is also the starburst shape that was used in building networks, e.g., in the form of tritopic, tetrahedral or octahedral nodes. Since each node in a net is necessarily in the starburst form (i.e., the connections emanate from each node outward onto the neighboring nodes), the backfolded shape presents a dilemma at first glance: if the molecule as a whole were to be treated as a
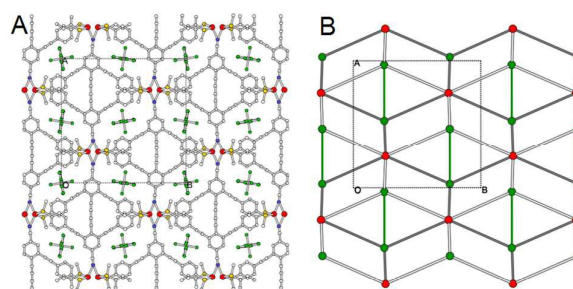
Fig. 4 A) A 2D network in the crystal structure of **3**-AgSbF$_6$. The Ag(I) ion is disordered over two sites. Red sphere, Ag; yellow, S; blue, N; green, F (from SbF$_6^-$). B) A schematic representation for highlighting the connectivity. The dark connections form a hexagonal net, and the lighter connections form a second one. Red sphere: average Ag position; green sphere: geometric center of the backbone benzene unit (i.e., the one bonded to the –CN groups) in molecule **3**; The green segment denotes the diacetylene group in **3**.

single node (as is normally the case in the design of molecular building blocks), the backfolded side arms would clearly not converge to give a single starburst nodal unit.
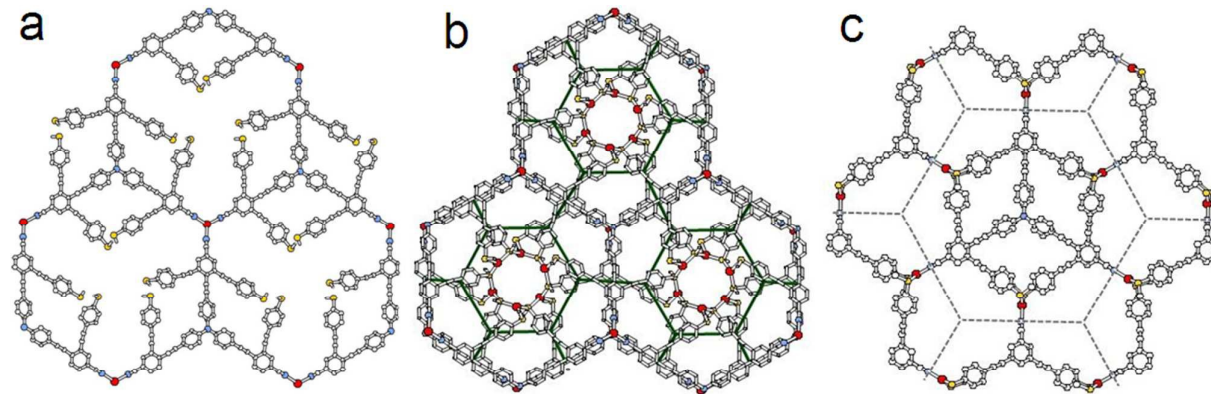
Fig. 5 The two types of networks in **4**-AgSbF$_6$. a) The primary net based on the coordination between the –CN groups and Ag$^+$ ions in the first type. b) A full view of the first type of network, containing two grids of (a) stacked together; the green grid traces the side arms and represents the secondary net that is hierarchically related to the primary net; the SbF$_6^-$ anions are omitted. c) The second type of network. Each Ag$^+$ bonds to two S atoms, and one –CN group. The dashed lines trace the empty hexagons and represent a higher-ordered grid. Color code: Ag, red; S, yellow; N, blue.

The dilemma can, however, be resolved by dissecting the molecule into subunits that conform to the starburst shape (e.g., the tritopic subunits in **3** and **4**), and then tracking the connection of the individual subunits in the resultant network.

The 2D net from molecule **3** and AgSbF$_6$ is illustrative. Fig. 4a shows the chemical linkage: the linear backbones was linked into a chain via the CN-Ag(I) bonds; the chains are integrated into the 2D net by the side arm methylthio (MeS-) groups that also bond to the Ag(I) centers. The prominent side arms thus give rise to a seemingly complex net. However, by focusing on the tritopic subunit (i.e., that of one cyano and two methylthio groups), one identifies two honeycomb nets that intersect at the Ag ions as well as interconnect via the diacetylene unit that is built into the molecules of **3** (Fig. 4b). As the two tritopic subunits of **3** each belong to a separate net, a clear mapping is thus established from the two tripods in the molecule of **3** to the two-net system in the solid state.

The hierarchical structure of **4** presents a more elaborate case for structural studies. It crystallized with AgSbF$_6$ to form an intriguing structure (**4**-AgSbF$_6$) consisting of two distinct layers that are alternately stacked.[18b] In one layer, the primary (-CN) branches bond to one set of Ag$^+$ ions to form a honeycomb net (the primary net, Fig. 5a). Each layer (Fig. 5b) contains two such honeycomb sheets stacked together, with the side arms (-SMe) bonded to a second set of Ag$^+$ ions, giving rise to a secondary honeycomb net. Taken together, the primary and secondary nets constitute a hexagonal hierarchy (Fig. 5b) that, interestingly, happens to be well-known in economic geography.[19]

In the other layer found in **4**-AgSbF$_6$, the –CN and the MeS- groups conjointly bind a single set of Ag(I) ions (Fig. 5), thus contrasting the above "division of labor" between the backbone and side arms. In other words, each –CN group and the two associated MeS- groups act jointly as a tritopic

subunit, and the molecule of **4** thus dissects into three subunits as such (which are preassembled by the triphenylamine core of **4**). In addition, the length of the MeS- side arms enables a chelation on the Ag(I) ions—i.e., the two MeS- groups around each Ag are from the same molecule of **4**. As a result, all the tritopic subunits are linked into a single honeycomb net. Interestingly, this honeycomb net also presents distinct hierarchical features: it contains two types of hexagons, one filled with the triphenylamine core and the other is empty; the distribution of the two hexagons follows the same hexagonal hierarchy as mentioned above (see also Fig. 5b).

To recap, the two types of networks in **4**-AgSbF$_6$ follow, respectively, from two distinct ways of dissecting molecule **4** into the conventional tritopic subunits. One is to treat the three –CN primary branches as a tritopic subunit, and the hierarchically related MeS- side arms were naturally grouped into a subsidiary honeycomb domain/net. The other way is non-hierarchical: i.e., to group each –CN branch and the two associated MeS- branches into a tritopic subunit, and consequently treat each molecule of **4** as three tritopic subunits that are preassembled by the triphenylamine core (Fig. 5c).

Is that it?—the backfolded shape is simply a bunch of star-
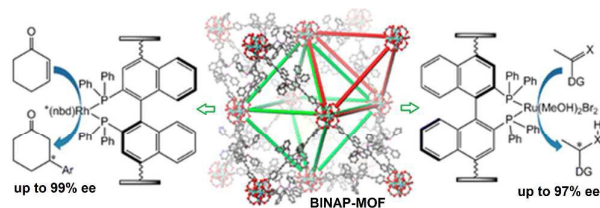
Fig. 6 A Zr(IV)-based BINAP-MOF and the enantioselective catalytic activities observed of its metalated analogs (Rh and Ru). The linker contains two linear –C≡C-C$_6$H$_4$-COOH units on a homochiral BINAPH core. Adapted with permission from Ref 11d. Copyright (2014) American Chemical Society.

ARTICLE

shape subunits stitched together? We venture to think that such a reductionist view is incomplete--after all, the backfolded shape is complex, hierarchical, and it presents fundamentally new features of molecular configuration. Such new features are well illustrated in the self-similar network structures formed by the Sierpinski molecule **4**. The following is a speculative idea. Because the star-shaped subunits are, perforce, conjoined by the covalent links (which assemble the backfolded molecule), the formation and arrangement of the subnets (each arising from a subset of the star-shaped subunits) are subject to the geometric and energetic constraints imposed by these links. We suspect that the interplay among the subnets and the constraints might, in some cases, cause packing frustration, and lead to novel phenomena of disordering and even incommensurate periodicity/quasicrystallinity among these organic-based solid state systems. More realistically, further studies can be conducted on backfolded molecules with various designs on the donor groups and backbone/side arm structures.[20] Incidentally, the pre-linked terephthalic acid ligands, found by the Cohen group to persistently converge into the prototypical MOF-5 net, can be compared with molecules **3** and **4**, further highlighting the pre-assembled character of these seemingly complex ligand structures.[21]

Sulfur side groups contrasting the backbone

Let us now move back to the more topical issue of functionalization, and make some choice as to the functions of the side group. The endless array of organic functions gives

medium of open frameworks, i.e., synergism giving rise to reactivities and properties that would not be normally accessible in the traditional settings of, e.g., solution chemistry and shake-and-bake solid state synthesis.

Contrast, on the other hand, gives some real guidance--a simple course of action is to contrast the chemical function of the backbone. For this, the hard-and-soft design is relevant. As a majority of MOFs are built on the hard, ionic carboxylate linkers, a chemically soft side group naturally comes to mind. A brief stare at the periodic table spots S and P as appealing choices, because of the bona fide softness as well as their very familiar chemistry (incidentally, any side group is bound to be somewhat different in hardness from the backbone—but it is by way of contrasting that S and P stand out as clear choices).

Indeed, the phosphine unit, in the hard-and-soft formation, has been explored for functionalizing MOF materials,[11] as is pioneered by Lin's earlier hybrid solid catalysts based on phosphine-phosphonate linkers.[11a] Also notable is the highly enantioselective, wide-scope catalysis by a class of homochiral BINAPH-MOFs recently invented in the same group (Fig. 6).[11d] In these systems, a synergism can be identified: the host grid imposes site isolation on the catalytic centers, thus serving to minimize intermolecular catalyst deactivation and enhance the catalytic activity.

Sulfur, being less prominent in catalysis, nevertheless offers advantages. For example, thioethers are stable to air, and can be conveniently tailored in length and shape—even to make as complex a structure as a dendrimer.[22] Curiously, though,
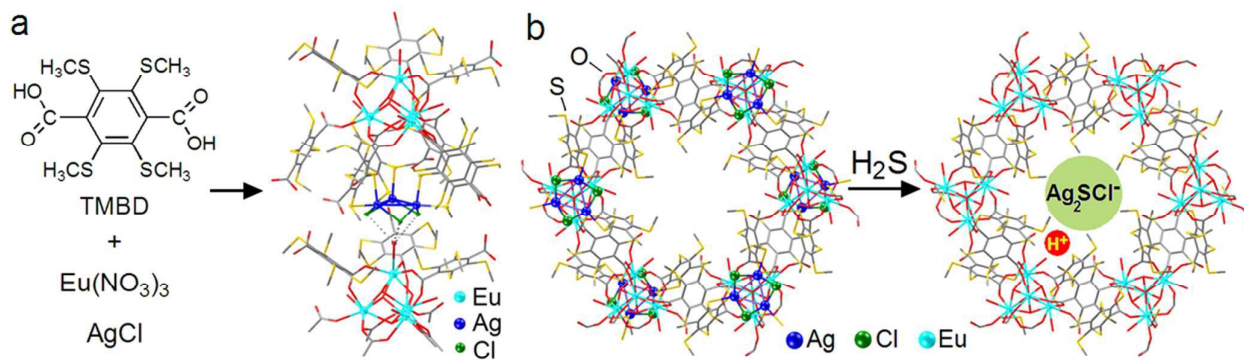
Fig. 7 a) The synthetic scheme of EuTMBD-AgCl, showing the local bonding features of the carboxyl-bound Eu_4O_4 cluster and sulfur-bound AgCl trimer in the X-ray single crystal structure. b) A view of the single crystal structures of EuTMBD-AgCl along the channel direction before (left) and after (right) treatment by H_2S gas: the EuTMBD host net holds up in the process, while the AgCl moiety reacts to form disordered Ag_2SCl^- (compositions can vary) species which are located at the central region of the channel.

freedom in theory but often bewilderment in practice, and the way of choosing is as rich as chemistry itself. In the spirit of rooting for the side group, we seek to promote the interaction and the contrast with the backbone. Interaction is often a vague fancy term with no real value of guidance, but here it helps sharpen the intent for unique synergism with the

thioether side groups reported to date remain mostly simple and small (e.g., $-SCH_3$ and $-SCH_2CH_2SCH_3$). By comparison, a thioether side chain with a more complex (e.g., dendritic) structure would be more imposing in appearance, and more stirring for the mind.
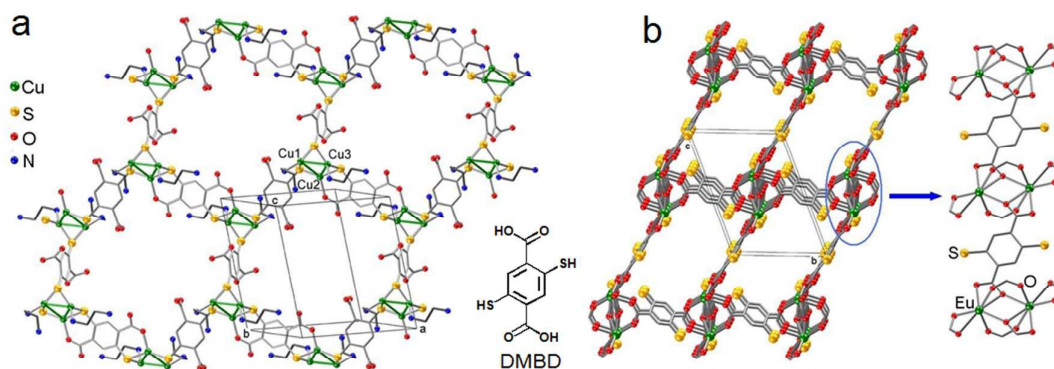
Fig. 8 a) An overview of the 2D network of CuDMBD: normal bonding distances (2.177 to 2.302 Å) are observed for all the six Cu-S contacts around the Cu(I) trimer. b) View of the 3D net of EuDMBD along the a axis, and the connection of the $Eu_2(COO)_6$ units shown along the a axis (right) to highlight the free-standing thiol units.

One major use of the thioether side group has been the uptake/trapping of soft metal guests (e.g., Ag^+, Hg^{2+}, Pd^{2+}), which opens opportunities for larger functional impacts. For example, the sulfur-bound AgCl moiety in the 3D net of EuTMBD-AgCl (crystallized from the hard-and-soft molecule TMBD, Eu^{3+} and AgCl; see Fig. 7)[23] can be reacted with H_2S, generating black sulfide nanoclusters which remain trapped in the upstanding host net.[‡] The broad functional impact of imbedding chalcogenide sub-domains (e.g., as quantum dots) within the MOF matrix is obvious, because of their rich electronic and photochemical properties. Moreover, by tailoring the pore features of the MOF host, as well as the thioether side chains, one can systematically control the

counterions apparently being the H^+ species resulted from the H_2S treatment. It remains of interest to explore the potential use of the acidic H^+ counterions, e.g., catalytic properties and proton conductivity.

The thiol function as the grand unifier

It appears as though we are drifting away from the central theme of merging the backbone and the side group. After all, the above chalcogenide sub-domains stand distinctly apart from the host frame, with relatively weak chemical links in between. On the other hand, these inorganic subdomains, introduced via the thioether donors, can outshine the backbone with their rich chemical and electronic properties, and vindicate, in a sense, the rising of the side group. Let us
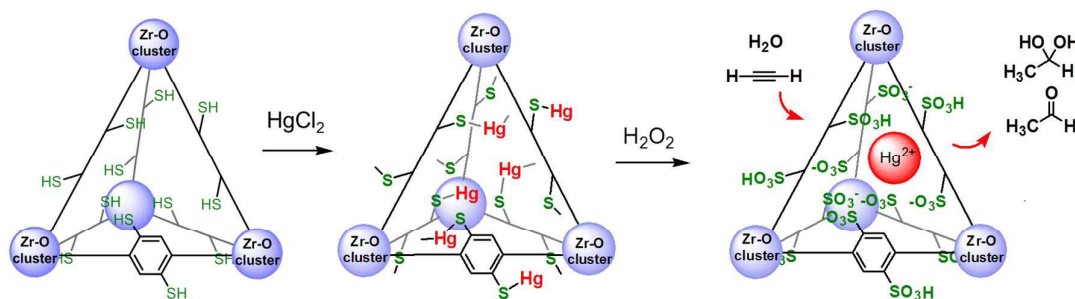
Fig. 9 Left: a schematic for the ZrDMBD network (left; same topology as UiO-66; simplified as a tetrahedral cage unit). Middle: the uptake of Hg species to install the covalent metal-thiolate links throughout the network; the electronic properties can thus be conveniently tuned by the diverse metal guests that can be entered to link up the thiol donors. Right: H_2O_2 oxidation generates acidic Hg^{2+} and H^+ ions that catalyses the hydration of acetylene.

size/shape of the metal chalcogenide sub-domain, and the associated reactivities and materials properties. For instance, one can aim to form a continuous subsidiary net of the chalcogenide for effective charge transport throughout the composite solid matrix.

Also notably, the reaction between H_2S and AgCl here does not convert all the Cl^- ions into gaseous HCl, and the remaining Cl^- ions presumably could stay bonded to the Ag(I) ions (e.g., possibly as a chlorosulfide species like Ag_2SCl^-), with the

now move on to the thiol function (-SH), which, because of its unique, rich reactivity, proves to be a powerful side group in the narration of merging and unification.

The groundwork was laid by a systematic study on the reticular chemistry of the molecule DMBD (2,5-dimercapto-1,4-benzenedicarboxylic acid).[13a] Two of the structures discovered therein were most relevant. In one (CuDMBD, Fig. 8a), all the sulfur atoms are bonded to the soft Cu(I) ions to build up a 2D thiolate grid featuring substantial electronic

interaction across the metal centers and the aromatic cores; while half of the carboxyl groups remain uncoordinated, serving, in an anecdotal role reversal, as the side group pending off the Cu(I)-thiolate grid. In the other (EuDMBD, Fig. 8b), the very hard Eu(III) coordinate selectively with the carboxyl groups to form a 3D MOF grid, while leaving the thiol groups as free-standing side groups that open the potential for metal uptake and for crosslink modifications.

Such potential was explored in a subsequent study[24] on the more robust ZrDMBD net (of the UiO-66 type[25]), which, with its free-standing thiol side groups, readily takes up mercury vapor as well as aqueous Hg(II) species. The simple treatment of Hg insertion serves to install the covalent Hg(II)-thiolate bridges across the ligands (cf. the siloxane links in Fig. 2) and impart extra stability to the MOF host. For example, the as-made ZrDMBD solid (prior to Hg uptake), like many Zr(IV)-based MOFs, is sensitive to F$^-$ ions (due its very strong hard-to-hard affinity for the Zr^{4+} centers), and instantaneously dissolves in a dilute NaF solution (e.g., 0.5% w/w); by contrast, the Hg-loaded solid ZrDMBD-Hg, even after being stirred in the same NaF solution for several days—with up to 45% of the Zr ions being extracted out of the host grid, retains the original crystalline order.

Moreover, the highly polarizable Hg(II)-thiolate links--or other transition metal-thiolate that can be conveniently installed this way—offer to electronically integrate the individual ligand π systems. The hard-and-soft design therefore

The leach-free catalysis enabled by the Pd atoms anchored by the thiol-tagged ZrDMTD net also reveals a remarkable synergism between the side group and the backbone (DM: dimercapto; TD: terphenyldicarboxyl; Fig. 10). Therein, the longer DMTD linker expands the framework, spacing farther apart the thiol groups: i.e., even the closest S···S distance being longer than 5.24 Å as measured from the single crystal structure. As a result, the Pd(II) center can fully bond with only one single thiol unit, leaving the coordination sphere open for catalysis. The spatial confinement imposed by the rigid grid thus thwarts the poisoning effect of thiols, an effect that is well-known in the solution phase, and can be ascribed to the free-flowing thiol molecules scrambling onto, and sealing off the Pd center with the intractable thiol-Pd bonds.

Moreover, the use of the dangling, isolated thiol groups to anchor Pd atoms effectively turns the intractable Pd-S bond on its head, as its very strength suppresses Pd leaching, and makes for durable heterogeneous catalysis. The leach-free, truly heterogeneous nature of the solid catalyst was rigorously characterized by two tests. In one test, two aryl iodide substrates were simultaneously deployed: one small and one big; while the small one readily enters into the pores, the big does not—it stays in the solution all the time. Only the small one was reacted, while the big one remained intact, indicating that, even amidst all the dynamics of the catalytic process for the small substrate, no Pd species was leached into the solution to convert the big substrate.
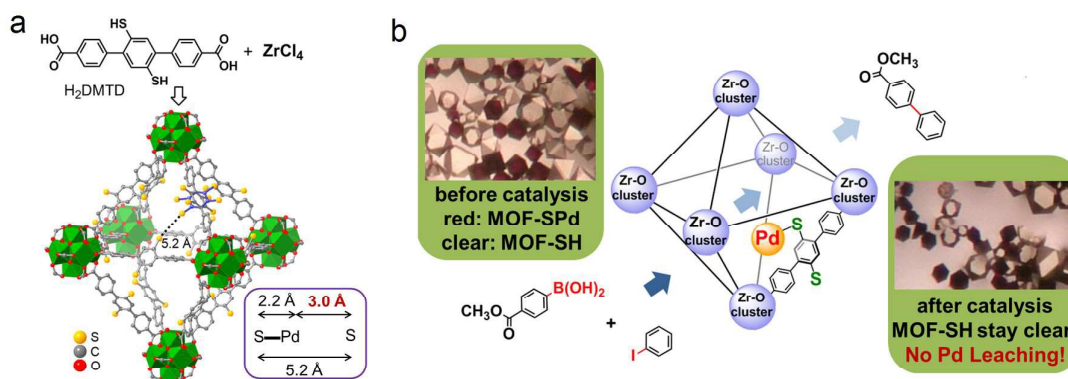
Fig. 10 a) Synthetic scheme for ZrDMTD, which is represented by an octahedral cage taken from the single crystal structure. The dotted line indicates a shortest S···S distance of 5.2 Å: as seen in the inset, a typical Pd-S bond at 2.2 Å gives 3.0 Å as the shortest distance the other S atoms can get to the Pd center. Disorder of the central benzene ring is shown in only one linker; Zr coordination polyhedra displayed in green; b) A schematic of Suzuki coupling reaction catalysed in the presence of both the the red, metallated ZrDMTD-Pd crystals and the colorless as-made crystals that were meant as a trap for Pd species, together with photographs of the reaction mixture before and after the reaction: the colorless as-made crystals show no color change, indicating that they did not get loaded with Pd in the reaction process—i.e., no Pd was leached from the colored metallated crystals.

offers a powerful divide-and-conquer solution to the assembly of the intractable metal-thiolate net. The wide-ranging organic π systems, coupled with the various metal-sulfur links that can thus be conveniently installed, offers an attractive platform for exploring reactivities and materials properties in the open framework medium (see also examples of H$_2$O$_2$ treatment to generate proton conductivity,[26] and the strong Lewis acid solid state catalysts in Fig. 9[27]).

The other test is based on lively color observations: the as-made MOF crystals (with free-standing –SH groups, denoted as MOF-SH) are almost colorless, and strongly fluorescent under UV radiation; upon being loaded with Pd (i.e., to form MOF-SPd), they take on a distinct red color, with the fluorescence being suppressed.

The colorless MOF-SH crystals were then added into a reaction system where the dark-red MOF-SPd crystals acted as

the catalyst. The design is clear: any Pd that leached out of the MOF-SPd crystals would then be trapped into the MOF-SH crystals (thanks to the strongly binding –SH groups therein), and trigger a red color as well as fluorescence quenching in the latter. Neither red color (Fig. 10) nor fluorescence quenching occurred to the MOF-SH crystals, strongly supporting the absence of Pd leaching from the colored MOF-SPd crystals.

While similar tests of these sorts are already known in the field of classical heterogeneous catalysis (e.g., as the three-phase test and the poison test, respectively),[28] they are especially relevant for the increasingly popular field of MOF catalysis, because many reported activities could arise from leached Pd species instead—such Pd species are formed as soluble, highly active species in situ, and yet they redeposit upon workup or filtration.[29] In view of the prevalent palladium leaching in the various supported systems,[29d] the ZrDMTD crystals provide an especially valuable platform for exploring and for rigorously examining leach-free, heterogeneous catalysts.

Outlook: functional flip-flop and sequential metal insertion

The far-apart thiol groups dotting the rigid host net, together with the subsequently anchored, open Pd centers, conjure up an image of functional flip-flop. To wit, the initial, as-made MOF host, with its free-standing thiol sites, sports strong donor character, as is evidenced in the effective uptake of the Pd(II) ions. By contrast, the Pd(II) ions tagged onto the solid grid, with their open, unsaturated coordination spheres, impart distinct Lewis acidity, which manifests itself in the robust catalytic activity demonstrated.

The basicity/acidity inversion can potentially be reiterated to generate a sequence of functional flip-flops: namely, the metallated MOF-S-Pd acid host can bond with small-size donors like S^{2-} or WS_4^{2-}, to fully seal up the Pd^{2+} center, and to revert to the Lewis base state [e.g., as MOF-S-Pd-$(S^-)_n$ or MOF-S-Pd-$(SWS_3^-)_n$; n can vary], which, in turn, can pick up Ag^+, Pd^{2+} or other metal ions to grow the sequence. The flip-flop of the acid-base states thus translates into a controlled, sequential insertion of the metal centers as well as the donor constituents. The ever larger pores (e.g., 8.5-nm aperture[30]) being achieved in the MOF hosts, especially in systems based on the very hard Zr(IV) or Mg(II) ions, provide ample space to deploy this strategy of sequential insertion, and to custom-build metal-chalcogenide bridges that closely integrate the organic π systems of the host grid. The metal-chalcogen (or other metal-donor) sub-domains, with their rich tunable compositions and properties that can be dialed in by the sequential insertion, present the new horizon of controlled solid state synthesis within the well-defined matrix of metal-organic frameworks.

Notes and references

‡ In spite of the drastic reaction with H_2S, which dislodges the AgCl cluster imbedded from the host net to forms Ag_2S species in the pore region, single crystal X-ray diffraction remains viable with the H_2S-treated crystals, which reveals the same host net connectivity as found in the initial, as-made sample. Moreover, the single crystal structure also indicates an empty pocket on the host net, which originally was occupied by the Ag_3Cl_3 trimer; while significant electron density peaks (disordered) were found in the pore region. These peaks amount to 752 electrons, and closely matches the guest content in the formula $[Eu_4(OH)_4(H_2O)_4]_2(C_{12}H_{12}O_4S_4)_9 \cdot 32H_2O \cdot 5.92H^+ \cdot 0.98[Ag_6S_3Cl_4]$ as determined by elemental analyses. I.e., $Ag_6S_3Cl_4^-$ and $32H_2O$ together contain 718 electrons, being slightly smaller than the 752 electrons from the single crystal structure, which can be ascribed to the different sample treatments: while the single crystal was never pumped on, the sample for elemental analysis was pumped under 140 ∘C for several hours (this might have removed some of the volatile guests). CCDC 1422534 contains the crystallographic data for the H_2S-treated EuTMBD-AgCl crystal.

1. C. Wang, D. Liu and W. Lin, *J. Am. Chem. Soc.*, 2013, **135**, 13222.
2. a) M. Simard, D. Su and J. D. Wuest, *J. Am. Chem. Soc.*, 1991, **113**, 4696; b) X. Wang, M. Simard and J. D. Wuest, *J. Am. Chem. Soc.*, 1994, **116**, 12119.
3. B. F. Hoskins and R. Robson, *J. Am. Chem. Soc.*, 1989, **111**, 5962.
4. G. B. Gardner, D. Venkataraman, J. S. Moore and S. Lee, *Nature* 1995, **374**, 792.
5. M. Kondo, T. Yoshitomi, K. Seki, H. Matsuzaka and S. Kitagawa, *Angew. Chem., Int. Ed. Engl.*, 1997, **36**, 1725.
6. O. M. Yaghi, M. O'Keeffe, N. W. Ockwig, H. K. Chae, M. Eddaoudi and J. Kim, *Nature*, 2003, **423**, 705.
7. a) G. Kumar and R. Gupta, *Chem. Soc. Rev.*, 2013, **42**, 9403; b) T. Muller and S. Braese, *RSC Adv.*, 2014, **4**, 6886; c) V. Guillerm, L. J. Weselinski, Y. Belmabkhout, A. J. Cairns, V. D'Elia, L. Wojtas, K. Adil and M. Eddaoudi, *Nat. Chem.*, 2014, **6**, 673; d) M. D. Wise, A. Ruggi, M. Pascu, R. Scopelliti and K. Severin, *Chem. Sci.*, 2013, **4**, 1658; e) M. Pascu, M. Marmier, C. Schouwey, R. Scopelliti, J. J. Holstein, G. Bricogne and K. Severin, *Chem. - Eur. J.*, 2014, **20**, 5592; f) P. Thanasekaran, T.-T. Luo, J.-Y. Wu and K.-L. Lu, *Dalton Trans.*, 2012, **41**, 5437; g) T.-H. Chen, I. Popov, W. Kaveevivitchai and O. S. Miljanic, *Chem. Mater.*, 2014, **26**, 4322.
8. a) Y.-H. Kiang, G. B. Gardner, S. Lee, Z. Xu and E. B. Lobkovsky, *J. Am. Chem. Soc.*, 1999, **121**, 8204; b) Y.-H. Kiang, G. B. Gardner, S. Lee and Z. Xu, *J. Am. Chem. Soc.*, 2000, **122**, 6871; c) Z. Xu, Y.-H. Kiang, S. Lee, E. B. Lobkovsky and N. Emmott, *J. Am. Chem. Soc.*, 2000, **122**, 8376; d) Z. Xu, S. Lee, Y.-H. Kiang, A. B. Mallik, N. Tsomaia and K. T. Mueller, *Adv. Mater.*, 2001, **13**, 637.

9. a) C.-D. Wu, A. Hu, L. Zhang and W. Lin, *J. Am. Chem. Soc.*, 2005, **127**, 8940; b) D. Rankine, A. Avellaneda, M. R. Hill, C. J. Doonan and C. J. Sumby, *Chem. Commun.*, 2012, **48**, 10328; c) K. L. Mulfort, O. K. Farha, C. L. Stern, A. A. Sarjeant and J. T. Hupp, *J. Am. Chem. Soc.*, 2009, **131**, 3866.

10. a) S. Henke, A. Schneemann, A. Wuetscher and R. A. Fischer, *J. Am. Chem. Soc.*, 2012, **134**, 9464; b) S. Henke, A. Schneemann and R. A. Fischer, *Adv. Funct. Mater.*, 2013, **23**, 5990.

11. a) A. Hu, H. L. Ngo and W. Lin, *J. Am. Chem. Soc.*, 2003, **125**, 11490; b) A. M. Bohnsack, I. A. Ibarra, V. I. Bakhmutov, V. M. Lynch and S. M. Humphrey, *J. Am. Chem. Soc.*, 2013, **135**, 16038; c) F. L. Morel, M. Ranocchiari and J. A. van Bokhoven, *Ind. Eng. Chem. Res.*, 2014, **53**, 9120; d) J. M. Falkowski, T. Sawano, T. Zhang, G. Tsun, Y. Chen, J. V. Lockard and W. Lin, *J. Am. Chem. Soc.*, 2014, **136**, 5213.

12. a) X.-P. Zhou, Z. Xu, M. Zeller, A. D. Hunter, S. S.-Y. Chui and C.-M. Che, *Inorg. Chem.*, 2008, **47**, 7459; b) A. D. Burrows, C. G. Frost, M. F. Mahon and C. Richardson, *Chem. Commun.*, 2009, 4218; c) J. He, K.-K. Yee, Z. Xu, M. Zeller, A. D. Hunter, S. S.-Y. Chui and C.-M. Che, *Chem. Mater.*, 2011, **23**, 2940.

13. a) J. He, C. Yang, Z. Xu, M. Zeller, A. D. Hunter and J. Lin, *J. Solid State Chem.*, 2009, **182**, 1821; b) T. Liu, J.-X. Che, Y.-Z. Hu, X.-W. Dong, X.-Y. Liu and C.-M. Che, *Chem. - Eur. J.*, 2014, **20**, 14090.

14. a) J. Bonnefoy, A. Legrand, E. A. Quadrelli, J. Canivet and D. Farrusseng, *J. Am. Chem. Soc.*, 2015, **137**, 9409; b) T. A. Makal, X. Wang and H.-C. Zhou, *Cryst. Growth Des.*, 2013, **13**, 4760; c) K. Gedrich, M. Heitbaum, A. Notzon, I. Senkovska, R. Froehlich, J. Getzschmann, U. Mueller, F. Glorius and S. Kaskel, *Chem. - Eur. J.*, 2011, **17**, 2099.

15. a) R. K. Deshpande, J. L. Minnaar and S. G. Telfer, *Angew. Chem., Int. Ed.*, 2010, **49**, 4598; b) D. J. Lun, G. I. N. Waterhouse and S. G. Telfer, *J. Am. Chem. Soc.*, 2011, **133**, 5806; c) R. K. Deshpande, G. I. N. Waterhouse, G. B. Jameson and S. G. Telfer, *Chem. Commun.*, 2012, **48**, 1574.

16. S. M. Cohen, *Chem. Rev.*, 2012, **112**, 970.

17. a) S. Lee, A. B. Mallik, Z. Xu, E. B. Lobkovsky and L. Tran, *Acc. Chem. Res.*, 2005, **38**, 251; b) Y. H. Kiang, S. Lee, Z. Xu, W. Choe and G. B. Gardner, *Adv. Mater.*, 2000, **12**, 767.

18. a) Y.-Q. Sun, J. He, Z. Xu, G. Huang, X.-P. Zhou, M. Zeller and A. D. Hunter, *Chem. Commun.*, 2007, 4779; b) Y.-Q. Sun, C. Yang, Z. Xu, M. Zeller and A. D. Hunter, *Cryst. Growth Des.*, 2009, **9**, 1663; c) Z. Xu, Y.-Q. Sun, J. He, M. Zeller and A. D. Hunter, in *The concept and use of a class of branchy molecules with centripetal self-similarity*, Nova Science Publishers, Inc., Hauppauge, NY 2008.

19. W. Christaller, *Central Places in Southern Germany*, Prentice Hall, Englewood Cliffs, 1966.

20. J. Cui, Y.-L. Wong, M. Zeller, A. D. Hunter and Z. Xu, *Angew. Chem., Int. Ed.*, 2014, **53**, 14438.

21. a) C. A. Allen, J. A. Boissonnault, J. Cirera, R. Gulland, F. Paesani and S. M. Cohen, *Chem. Commun.*, 2013, **49**, 3200; b) Z. Zhang, H. T. H. Nguyen, S. A. Miller and S. M. Cohen, *Angew. Chem., Int. Ed.*, 2015, **54**, 6152.

22. a) R. Hoogenboom, *Angew. Chem., Int. Ed.*, 2010, **49**, 3415; b) A. B. Lowe, C. E. Hoyle and C. N. Bowman, *J. Mater. Chem.*, 2010, **20**, 4745; c) A. Dondoni, *Angew. Chem., Int. Ed.*, 2008, **47**, 8995; d) H.-F. Chow, M.-K. Ng, C.-W. Leung and G.-X. Wang, *J. Am. Chem. Soc.*, 2004, **126**, 12907.

23. X.-P. Zhou, Z. Xu, M. Zeller, A. D. Hunter, S. S.-Y. Chui, C.-M. Che and J. Lin, *Inorg. Chem.*, 2010, **49**, 7629.

24. K.-K. Yee, N. Reimer, J. Liu, S.-Y. Cheng, S.-M. Yiu, J. Weber, N. Stock and Z. Xu, *J. Am. Chem. Soc.*, 2013, **135**, 7795.

25. J. H. Cavka, S. Jakobsen, U. Olsbye, N. Guillou, C. Lamberti, S. Bordiga and K. P. Lillerud, *J. Am. Chem. Soc.*, 2008, **130**, 13850.

26. W. J. Phang, H. Jo, W. R. Lee, J. H. Song, K. Yoo, B. S. Kim and C. S. Hong, *Angew. Chem., Int. Ed.*, 2015, **54**, 5142.

27. K.-K. Yee, Y.-L. Wong, M. Zha, R. Y. Adhikari, M. T. Tuominen, J. He and Z. Xu, *Chem. Commun.*, 2015, **51**, 10941.

28. a) J. D. Webb, S. MacQuarrie, K. McEleney and C. M. Crudden, *J. Catal.*, 2007, **252**, 97; b) I. W. Davies, L. Matty, D. L. Hughes and P. J. Reider, *J. Am. Chem. Soc.*, 2001, **123**, 10139; c) J. Rebek and F. Gavina, *J. Am. Chem. Soc.*, 1974, **96**, 7112.

29. a) N. T. S. Phan, M. Van Der Sluys and C. W. Jones, *Adv. Synth. Catal.*, 2006, **348**, 609; b) J. M. Richardson and C. W. Jones, *J. Catal.*, 2007, **251**, 80; c) M. Weck and C. W. Jones, *Inorg. Chem.*, 2007, **46**, 1865; d) A. N. Kashin, O. G. Ganina, A. V. Cheprakov and I. P. Beletskaya, *ChemCatChem*, 2015, **7**, 2113.

30. H. Deng, S. Grunder, K. E. Cordova, C. Valente, H. Furukawa, M. Hmadeh, F. Gandara, A. C. Whalley, Z. Liu, S. Asahina, H. Kazumori, M. O'Keeffe, O. Terasaki, J. F. Stoddart and O. M. Yaghi, *Science*, 2012, **336**, 1018.